Applied Human Factors and Ergonomics (AHFE2025), Vol. 199, 2025, 798–807
https://doi.org/10.54941/ahfe1006892

Development of a Wearable EEG Device Toward BCI Applications

Hisaya Tanaka and Sodai Kondo

Informatics Major, Kogakuin University Graduate School, Hachioji, TYO 192-0015, Japan

ABSTRACT

Electroencephalogram (EEG) technology is widely explored for applications in healthcare, disability assistance, and brain-computer interfaces. However, EEG devices commonly used in laboratories are often expensive and lack portability. In this study, we developed and evaluated an inexpensive, wearable EEG device as an alternative to the high-performance but immobile EEG1000 system. The proposed device employs a differential amplifier circuit with passive electrodes and consists of a single-channel analog front end, along with a digital section for analog-to-digital conversion and wireless transmission to a personal computer via Bluetooth low energy. It operates with a passband of 0.159–100 Hz, a sampling rate of 1 kHz, and 16-bit resolution within a 0–3.3 V range. Transient, alternating current, and noise analyses, as well as the common-mode rejection ratio, were evaluated using a simulator. Alpha waves were recorded under eyes-open and eyes-closed conditions, and the expected decrease and increase in alpha activity, respectively, were observed across 11 participants. However, the alpha response was more distinctly detected with the EEG1000 system. Future improvements will focus on enhancing performance by incorporating active electrodes and multichannel configurations.

Keywords: Wearable device, Electroencephalogram, Brain–computer interface

INTRODUCTION

An electroencephalogram (EEG) measures the brain activity from the scalp (Naydenov et al., 2022). It is investigated for diverse applications, including medical diagnosis, disability support, and brain–computer interfaces (BCIs). A BCI translates user intentions into computer commands by analyzing brain activity (Vidal, 1973). Devices commonly used to record EEG for experimental purposes are typically expensive and lack portability. In our previous studies, we used the costly and immobile EEG1000 system (Kondo and Tanaka, 2023; Kondo and Tanaka, 2025). However, in this study, we developed and evaluated an inexpensive, wearable EEG device as an alternative to EEG1000. Portable EEG devices make it possible to collect data from physically challenged individuals who have difficulty visiting research facilities. They also allow recordings in more practical settings, such as long-term daily monitoring. Moreover, when such devices are affordable, multiple units can be procured on a limited budget, thereby increasing the number of participants that can be included in a study. Therefore, in this work, we

develop a low-cost, wearable EEG device and present an initial performance evaluation by comparing it with EEG1000. The evaluation includes circuit simulations using SPICE software and alpha wave measurements under eyes-open and eyes-closed conditions.

EEG DEVICE SYSTEM

A wearable EEG device must be wirelessly connected and battery-powered; therefore, the proposed device is powered by Bluetooth low energy (BLE) communication and contains a LiPo battery. Figures 1 and 2 show the block diagram of the EEG device and the EEG device used in this study, respectively. The EEG device comprises electrodes, analog circuits, digital circuits, and a battery.

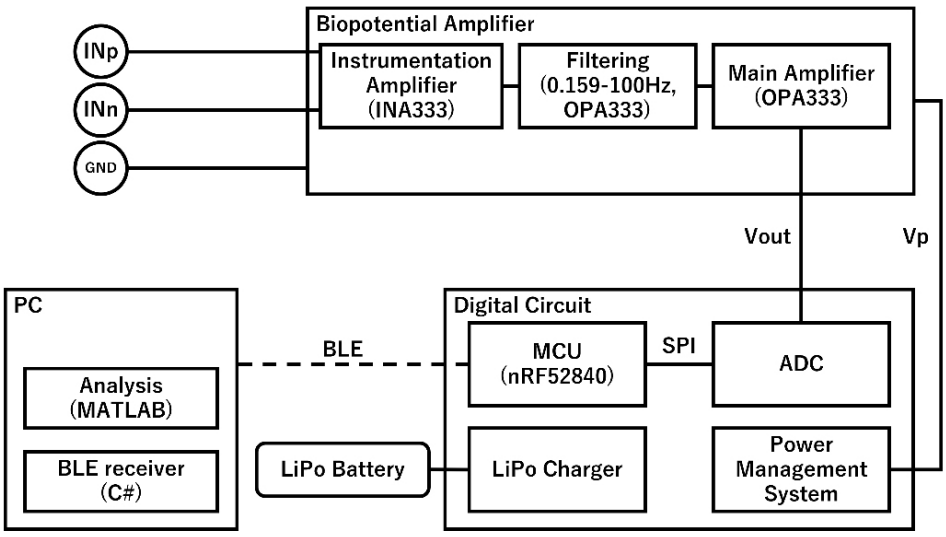

Figure 1: Block diagram of EEG device.

The BLE communication data sent from the EEG device were received by a C# program developed for Windows 11. The C# program sent the data in a streaming format via TCP to MATLAB for analyzing and recording the data.

Biopotential Amplifier

As shown in Figures 1 and 2, the biopotential amplifier in the EEG device amplifies weak signals while suppressing noise. Biopotentials, including EEG, are often affected by low-frequency noise from power lines and electrode cable motion. The impedance imbalance at the skin surface and the insufficient electrode input impedance can also degrade the signal quality (Yoo et al., 1995). Therefore, the EEG amplifiers require a high common-mode rejection ratio (CMRR), a high input impedance, and carefully designed filters. Herein, we designed a biopotential amplifier to satisfy these requirements. The schematic of the amplifier is shown in the "Biopotential Amplifier" section of Figure 1. The amplifier records EEG by amplifying the

voltage difference between the measurement and reference electrodes. The CMRR mainly depends on the instrumentation amplifier.

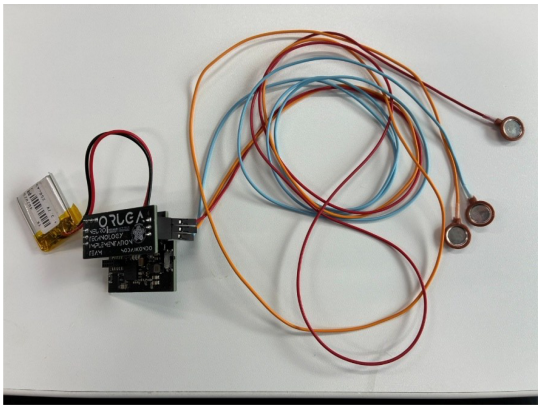

Figure 2: EEG device used in this study.

Typical EEG amplitudes fall in the range of about 15–150 μV within 0.5–30 Hz, with average values usually between 30 and 80 μV (Naydenov, 2022). In both EEG1000 and our measurement environment, the EEG amplitude was $\sim$10 μV; therefore, the expected amplitude was set to $\geq$10 μV. EEG must be amplified to exceed the noise levels and match the resolution of the analog-to-digital (A/D) converter. Herein, the A/D converter had a 16-bit resolution over a 0–3.3 V input range. The least significant bit (LSB) was calculated, as expressed in Eq. (1).

$$LSB = \frac{Range}{2^{ADCbit}} \tag{1}$$

With a 3.3 V reference and 16-bit resolution, the LSB value was 50.35 μV. Given a typical gain of 1000, an EEG signal of 10 μV was amplified to $\sim$10 mV. The ratio of the LSB to the amplified signal range was 0.5035%, which was sufficiently small. Accordingly, the total gain of the amplifier was set to $\sim$1000, implemented as a two-stage configuration with gains of 20 and 50 in the first and second stages, respectively. The exact gain may vary due to component tolerances and procurement conditions.

Filtering was applied in both the analog and digital stages. The analog front end provided a bandpass of 0.159–100 Hz. During MATLAB analysis, a 50 Hz notch filter and an 8–14 Hz bandpass filter was applied for alpha wave detection. The high CMRR of the instrumentation amplifier effectively suppressed the 50 Hz noise present at both the measurement and reference electrodes. The analog filter design emphasized group delay characteristics to preserve waveform shape. The power supply conditions and the op-amp slew rate were verified using Analog Devices' Filter Wizard, and the final active filter design was partially adjusted based on component availability. A Texas Instruments OPA333 operational amplifier was also used.

Digital Circuit

The digital circuit supplied power to the biopotential amplifier and transmitted its data output via BLE. An overview of the digital circuit is provided in the "Digital Circuit" section of Figure 1. As shown in Figure 1, the digital circuit comprised a microcontroller unit (MCU), a wireless communication module, an external A/D converter, a DC–DC regulator for power supply, and a LiPo battery charging module. The nRF52840 MCU was used and its peripheral design followed Nordic's reference guide (Nordic Semiconductor, 2024). Because the nRF52840 lacked a built-in A/D converter with sufficient speed and resolution for EEG signals, an external A/D converter was required. Data transmission between the A/D converter and the nRF52840 was implemented using SPI communication. A DC–DC regulator provided stable power from a 3.0–4.2 V LiPo battery. The LiPo battery, with a capacity of 350 mAh, required 2 h and 20 min for a full charge. The final digital circuit operated with a sampling rate of 1 kHz, a resolution of 16 bits, a signal range of 0–3.3 V, and a supply voltage of 3.3 V.

EVALUATION AND EXPERIMENT

Evaluation Using the Spice Simulator

We used PSpice for TI to design and simulate a biopotential amplifier. The simulation primarily comprised transient, alternating current (AC), and CMRR analyses. Other analyses included parametric analysis for component standardization and Monte Carlo analysis to assess component manufacturing errors.

The transient analysis investigated how the output voltage changes over time. The test input was simulated with positive and negative inputs of 10 and 0 V, respectively. Therefore, the output was expected to be ~10 mV based on the amplifier circuit gain. However, the analog circuit operated on a single power supply in the 0–3.3 V range; thus, the midpoint was ~1.65 V. Accordingly, the actual operating range was $\sim 1.65 \pm 0.01$ V. The AC analysis showed the output voltage and phase information for each frequency. Further, we focused on the waveform reproducibility and evaluated the linear phase response or group phase. The AC analysis analyzed the 0.01–1 kHz range and evaluated gain and group phase for each frequency.

CMRR represents the ability of an amplifier to reject in-phase signals. It is determined by comparing the amplifier's output for a common-mode input with its output for a differential input. The CMRR calculation formula is expressed in Eqs. (2) and (3) (Dabbaghian et al., 2024).

$$A = \frac{V_{out}}{V_{in}} \tag{2}$$

$$CMRR = 20 \log_{10} \left(\frac{A_{diff}}{A_{cm}} \right) \tag{3}$$

In the above equations, A represents the overall amplifier gain, A_{diff} represents the gain when an out-of-phase signal is input, and A_{cm} represents the gain when an in-phase signal is input. CMRR is generally expressed

in dB and converted to a logarithmic scale. An ideal differential amplifier completely rejects in-phase signals. In practice, however, small residual signals appear at the output, depending on the design of the instrumentation amplifier and associated circuitry. As a result, the CMRR has a finite value. In this study, we focused on ensuring appropriate transient and AC responses in terms of amplitude and frequency. CMRR was improved by minimizing mismatches in the electronic components associated with the positive and negative electrodes.

Alpha Wave Measurement

Spontaneous EEG is a type of EEG that occurs continuously, regardless of external stimuli or actions such as recalling motor imagery. An alpha wave is a type of spontaneous EEG and was discovered by Berger in 1929. Alpha waves are dominant in the 8–14 Hz range when the eyes are closed or during rest. They are predominant in the parietal and occipital regions, particularly in the occipital regions (Adrian, 2010). As an initial EEG test, herein, we compared the EEG device and EEG1000 using alpha wave measurements with eyes open and closed.

Figure 3 shows the electrode positions of the EEG device worn by the participant. The electrode positions were determined based on the extended 10–20 method recommended by the International Federation of Clinical Neurophysiology Societies (Nuwer, 1998). For both the EEG device and EEG1000, the measurement electrode was placed at Poz, with Fpz as the ground. The reference electrode was A1 for EEG1000 and A2 for the EEG device.

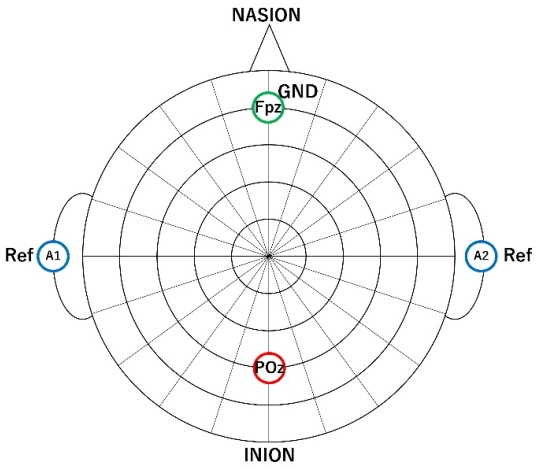

Figure 3: Measurement area.

Measurements were taken five times, each lasting 10 s with the eyes open and closed. The analog output of EEG1000 was transferred to a personal computer via a National Instruments USB-6218 device, while data from the EEG device were transferred via the BLE communication system described

earlier. All measurement data were integrated and saved using MATLAB. The study involved 11 male participants aged 21–25 years, all affiliated with Kogakuin University. The experiment was conducted in accordance with Kogakuin University's human research ethics review, titled "Development of Communication Assistive Technology for Patients with Aphasia and Neurological Disorders 2022-A-31." Participants were informed about the study and provided written consent.

RESULT

Spice Simulation

Figures 4–6 display the simulation results using PSpice for TI. Figure 4 shows the transient analysis. Figure 5 depicts the AC analysis. Figure 6 demonstrates the CMRR results.

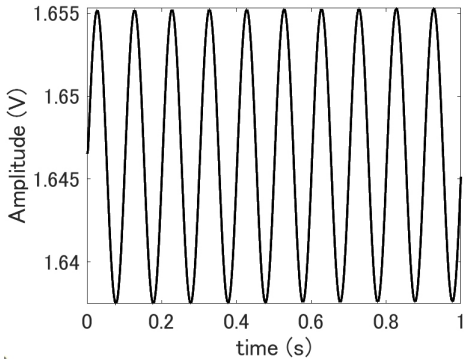

Figure 4: Transient analysis (10 Hz, 10 μV).

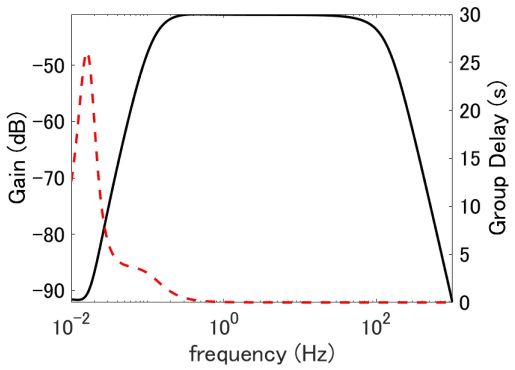

Figure 5: AC analysis (0.01–100 Hz).

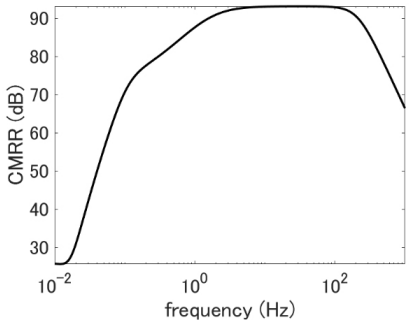

Figure 6: CMRR (dB).

Comparison of Alpha Waves Using EEG Device

Figure 7 shows alpha waves with the eyes open and closed for each subject using EEG1000. Figure 8 shows alpha waves with eyes open and closed for each subject using the EEG device. An analysis was performed using a 50 Hz notch filter and an 8–14 Hz bandpass filter, followed by an FFT to obtain alpha wave power values.

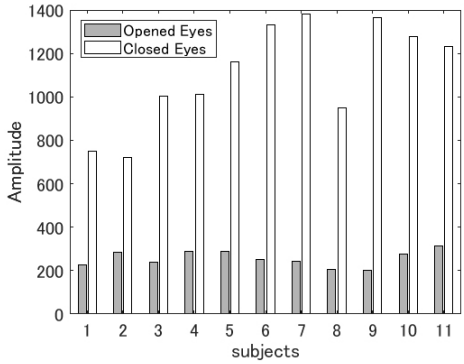

Figure 7: Alpha wave component by subject (EEG1000).

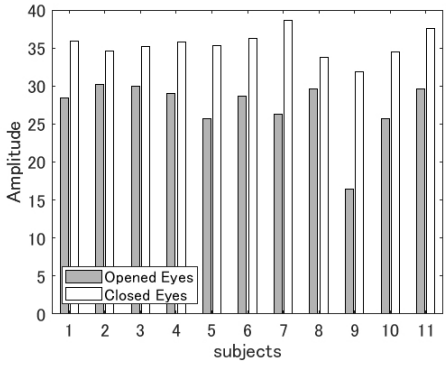

Figure 8: Alpha wave component by subject (EEG device).

DISCUSSION

EEG Device Performance Evaluation

The EEG device operation was confirmed through simulations using SPICE software and alpha wave measurements with the eyes open and closed. As shown in Figures 4–6, the EEG device demonstrates the required transient response, AC response, and CMRR. In particular, the expected values were obtained for the transient and AC responses, indicating that the analog circuit shown in Figures 1 and 2 is likely to function as intended. The CMRR shown in Figure 6 was relatively low, with a maximum of 93.16 dB, and therefore requires improvement. Since a driven right leg (DRL) circuit can enhance CMRR, future work will focus on applying a DRL circuit (Winter et al., 1983). In addition to confirming circuit operation in SPICE, the alpha wave components observed under eyes-open and eyes-closed conditions (Figure 8) indicate that the EEG device successfully detects alpha waves. In this study, alpha waves were measured using a single-channel EEG device; however, clearer detection is expected when the entire occipital region is monitored with a multichannel device. Accordingly, we plan to develop multichannel EEG devices in future work. Although the overall architecture requires further consideration, a multiplexer-based multichannel configuration appears preferable when cost efficiency is important. Based on these findings, the EEG device developed here demonstrates reliable simulation performance and effective alpha wave detection.

Comparison of EEG1000 and EEG Device and Performance Improvement

This section presents a comparison of EEG1000 and the EEG device. Both EEG monitors showed higher amplitudes with eyes closed and lower amplitudes with eyes open (Figures 7 and 8). However, EEG1000 showed less subject-to-subject variability and clearly detected differences in alpha waves with eyes open and closed, while the newly developed EEG device exhibited greater variability and a lower absolute magnitude. The output voltages are difficult to compare directly because the monitor's total gain also depends on the analog output range of EEG1000. Nevertheless, EEG1000 consistently demonstrated superior variability and alpha wave ratios between eyes-open and eyes-closed conditions, suggesting that the EEG device was slightly unstable. These results may be attributed to the reduced CMRR caused by the absence of a DRL circuit, as well as to differences in the induction methods of the two monitors. EEG1000's differential amplifier uses a system reference based on channels C3 and C4, which improves noise resistance, whereas the EEG device relies on simple differential amplification, making it more susceptible to imbalances in electrode contact impedance. Because both systems use the same electrode technology, the differences after the analog circuitry are evident in Figures 7 and 8.

Measures to improve the EEG device include implementing a DRL circuit and adopting a multichannel configuration. Another approach is the use of active electrodes, which enhance signal quality by incorporating a buffer amplifier to convert impedance. However, active electrodes can reduce

CMRR owing to additional wiring and component variations between electrodes; thus, their performance must be carefully evaluated through control experiments with and without implementation. Based on these results, the EEG device developed in this study was successful in detecting alpha waves but did not perform as a complete replacement for EEG1000. We aim to establish it as a substitute for specific applications by further enhancing its functionality and improving signal quality.

CONCLUSION

Herein, we developed and evaluated a cost-effective, wearable EEG device as an alternative to the expensive and less portable EEG1000. The proposed device was designed for single-channel operation with BLE communication and battery power, and it was evaluated using SPICE simulations and alpha wave measurements under eyes-open and eyes-closed conditions. The SPICE simulations demonstrated the expected transient and AC responses, achieving a maximum CMRR of 93.16 dB in the 0.159–100 Hz range. Although the device successfully detected alpha wave increases and decreases, its signal quality was poor compared to that of EEG1000, leaving room for improvement. Future work will focus on enhancing performance through multichannelization, DRL circuitry, and active electrodes, as well as tailoring its use to specific applications such as epilepsy prediction. Based on these findings, the developed EEG device successfully detected alpha waves and demonstrated basic functionality as an inexpensive, wearable alternative to EEG1000.

ACKNOWLEDGMENT

This work was supported by the Shotoku Science Foundation Grant.

REFERENCES

Adrian, E. D. and Matthews, B. H. C. (1934), The Berger Rhythm: Potential Changes From the Occipital Lobes in Man, Brain, 54(7), pp. 413–414.

Dabbaghian, A., et al. (2024), A 0.67 μ V-IIRN super-T Ω -Z IN 17.5 μ W/Ch Active Electrode With In-Channel Boosted CMRR for Distributed EEG Monitoring, IEEE Transactions on Biomedical Circuits and Systems, 18(1), pp. 3–15.

Kondo, S. and Tanaka, H. (2023), Improvement of the Accuracy of SSVEP-BCI with In-Ear EEG Using Multiple Regression Analysis, Neuroergonomics and Cognitive Engineering, AHFE2023, 102, pp. 264–273.

Kondo, S. and Tanaka, H. (2025), Performance Improvement of Ear-EEG SSVEP-BCI Using Reliability Score, Artificial Life and Robotics, 30, pp. 449–457.

Naydenov, C., Yordanova, A. and Mancheva, V. (2022), Methodology for EEG and Reference Values of the Software Analysis, Open Access Maced J Med Sci, 10(B), pp. 2351–2354.

Nordic Semiconductor (2024), nRF52840 Product Specification Reference Circuitry, 18 August 2025 viewed.

Nuwer, M. R., et al. (1998), IFCN standards for digital recording of clinical EEG, Electroencephalography and clinical Neurophysiology, 106(3), pp. 259–261.

Vidal, J. J. (1973), Toward direct brain-computer communication, Annual review of Biophysics and Bioengineering, 2(1), pp. 157–180.
Winter, B. B. and Webster, J. G. (1983), Driven-Right-Leg Circuit Design, IEEE Transactions on Biomedical Engineering, 30(1), pp. 62–66.
Yoo, S. K., et al. (1995), The Development of High Precision EEG Amplifier for the Computerized EEG Analysis, Proceedings of 17th International Conference of the Engineering in Medicine and Biology Society, pp. 1651–1652.